Reduction of Large Detailed Chemical Kinetic Mechanisms for Autoignition Using Joint Analyses of Reaction Rates and Sensitivities

A. SAYLAM,[1] M. RIBAUCOUR,[2] W. J. PITZ,[3] R. MINETTI[1]

[1] *PhysicoChimie des Processus de Combustion et de l'Atmosphère*, UMR CNRS/8522, *Université d'Artois*, *Porte Nord*, 62700 *Bruay-la-Buissière*, *France*
[2] *PhysicoChimie des Processus de Combustion et de l'Atmosphère*, UMR CNRS/8522, *Université des Sciences et Technologies de Lille*, 59655 *Villeneuve d'Ascq cedex*, *France*
[3] *Lawrence Livermore National Laboratory*, *Livermore*, CA 94551, USA

Received 17 March 2006; revised 1 August 2006, 23 September 2006, 8 November 2006; accepted 8 November 2006

DOI 10.1002/kin.20232
Published online in Wiley InterScience (www.interscience.wiley.com).

ABSTRACT: This study describes a new technique of reduction of detailed mechanisms for autoignition. It is based on two analysis methods. An analysis of reaction rates is coupled to an analysis of reaction sensitivity for the detection of redundant reactions. Thresholds associated with the two analyses have a great influence on the size and efficiency of the reduced mechanism. Rules of selection of the thresholds are defined. The reduction technique has been successfully applied to detailed autoignition mechanisms of two reference hydrocarbons: *n*-heptane and isooctane. The efficiency of the technique and the ability of the reduced mechanisms to reproduce well the results generated by the full mechanism are discussed. A speedup of calculations by a factor of 5.9 for *n*-heptane mechanism and by a factor of 16.7 for isooctane mechanism is obtained without losing accuracy of the prediction of autoignition delay times and concentrations of intermediate species. © 2007 Wiley Periodicals, Inc. Int J Chem Kinet 39: 181–196, 2007

INTRODUCTION

Improvement of combustion efficiency and minimization of pollutant emissions motivates research on advanced engine concepts such as homogeneous

Correspondence to: M. Ribaucour; e-mail: marc.ribaucour@univ-lille1.fr.

charge compression ignition (HCCI). Understanding of physical and chemical processes involved in the combustion of engine fuels is needed to predict onset of autoignition, oxidation rate, heat release rate, flame extinction, and concentration of species produced during the combustion. The chemical kinetics of fuel oxidation and autoignition plays a critical role in the HCCI concept.

Detailed chemical kinetic mechanisms have been developed to describe the oxidation of hydrocarbons. These mechanisms are very large in terms of numbers of species and reactions, and their size increases with the size of the hydrocarbon. For example, the GRI-Mech 3.0 mechanism of methane includes 52 species and 325 reactions [1]. The mechanism of butane elaborated by Pitz and Westbrook at Lawrence Livermore National Laboratory contains 140 species and 807 reactions [2]. In the mechanism of the three isomers of pentane built at the same laboratory, the submechanism of *n*-pentane alone is composed of 193 species and 975 reactions [3]. The mechanism of *n*-heptane worked out by Curran et al. contains 545 species and 2446 reactions [4], and the mechanism of isooctane by the same authors includes 858 species and 3606 reactions [5].

Because of their hierarchical mode of construction, detailed mechanisms of large hydrocarbons contain many species and reactions that are not needed for simulating ignition phenomena over the range of parametric conditions they are intended to cover. These redundant species and reactions needlessly raise the computational time or central processing unit (CPU) time of reacting flow simulations that use detailed mechanisms. When large mechanisms are employed, substantial computational resources are required even for zero-dimensional calculations. The size of large mechanisms impacts the time needed to perform reaction-path and sensitivity analyses, which are used to provide valuable insight into processes controlling the ignition of the fuel, the production of pollutant emissions, and the interpretation of experimental results. Reduced mechanisms are needed for use in one-dimensional (1D) flame calculations because present solvers are often unable to find solutions when large mechanisms are employed. For example, a reduced mechanism of *n*-heptane, deduced from the original mechanism of Curran et al., was used in studies of extinction and autoignition in counterflow configuration, which requires a 1D solver [6].

Practical fuels, such as gasoline and diesel fuels used in automotive engines, are made of hundreds of hydrocarbons belonging to four families: alkanes, alkenes, aromatics, and napthenes. Surrogate fuels composed of a limited number of hydrocarbons representing each family are important in ongoing and future research devoted to the emissions of automotive pollutants. The building of the mechanism of a surrogate fuel by gathering detailed mechanisms of individual hydrocarbons will lead to a final mechanism of enormous size, which would require extensive computational resources even for zero-dimensional calculations. In the case of multidimensional simulations in which computational fluid dynamics (CFD), heat transfer, and mass transfer are coupled with chemistry, the use of a detailed mechanism is precluded because CFD calculations alone are already very computationally intensive [7,8].

For all the reasons given above, it is necessary to use any available technique to produce reduced mechanisms able to reproduce the predictions of detailed mechanisms. A reduction technique has to decrease the number of reactions but mostly the number of species because the memory resources and the computational time increase with the number of differential equations solved by the kinetic code. Indeed, one differential conservation equation is associated with each species. It is well known that large mechanisms always admit some degree of redundancy when used for a particular application. Rejecting redundancy is the fundamental principle of a reduction technique.

Tomlin and coworkers wrote a comprehensive review about reduction techniques applied to combustion mechanisms [8]. Earlier, Griffiths proposed a review dedicated to reduced kinetic models, but the purpose of his review was broader and a priori reduced models as the Shell model and the Hu and Keck models are also described [9].

There are many different mathematical methods for reducing detailed mechanisms. However, they can be classified into three families depending on the more or less important chemical character maintained in the description of the mechanism after reduction. (i) The chemical family includes techniques such as the interspecies atomic flow analysis [10,11], the analysis of reaction and heat release rates [12], the different types of sensitivity analysis [13,14] and their coupling with the principal component analysis [15], the method of directed relation graphs [16–18], the method of directed relation graphs with error propagation [19], an optimization-based approach for obtaining optimally reduced mechanisms by reaction elimination [20], and an associated method for finding rigorous valid ranges for optimally reduced mechanisms [21]. (ii) The chemico-mathematical family is composed of techniques such as quasi-steady state approximation [22,23], partial equilibrium assumption, computational singular perturbation [24], and species lifetime analysis [25,26]. (iii) The mathematical family gathers the

repro-modeling technique [27] and the intrinsic low-dimensional manifold technique [28].

Few reduction techniques of the chemical family have been applied so far to a detailed mechanism that includes low ($T < 1000$ K) and high ($T > 1000$ K) temperature combustion chemistry for a large hydrocarbon, to the exception of the analysis of reaction and heat release rates [29,30]. We present a new reduction technique, which is able to build automatically the reduced mechanism after detection of unneeded species and reactions. The technique was developed with three aims: (i) to reduce rapidly and with a minimal human intervention large detailed mechanisms, (ii) to build mechanisms for surrogate engine fuels by combining reduced mechanisms of individual hydrocarbons, and (iii) to reduce the detailed mechanism of a mixture of hydrocarbon isomers and to extract a submechanism for one component of the mixture. This study describes how the first aim was reached.

The reduction technique is presented and its principle is described. Two methods are combined and used to detect redundant reactions. The choice of thresholds associated with the two methods and its influence on the size and efficiency of the reduced mechanism is discussed. Finally, the validation of reduced mechanisms for the two reference hydrocarbons—*n*-heptane and isooctane—is presented.

PRESENTATION OF THE TECHNIQUE

Principle of the Reduction Technique

Redundant reactions are recognized by two methods: the analysis of reaction rates and the analysis of sensitivity. The first analysis divides the entire reaction set into two: a group of slow reactions and a group of fast reactions. The analysis of sensitivity also divides the entire reaction set into two: a group of rate-limiting reactions and a group of non–rate-limiting reactions. The results of both analyses are coupled to identify the redundant reactions. They are non–rate-limiting slow reactions. Once the redundant reactions are recognized, the redundant species are identified as the species taking part solely in redundant reactions. Finally, the reduced mechanism is obtained by removing all redundant reactions and redundant species from the full mechanism.

To predict the chemistry of autoignition of hydrocarbons, the two analyses are performed using the results of a unique simulation of the autoignition of a mixture hydrocarbon/O_2/diluent in a rapid compression machine or in a shock tube with a detailed mechanism. The simulations are carried out with the chemical kinetic code SENKIN [31] associated with the package CHEMKIN-II [32] by considering an adiabatic and homogeneous system of constant volume.

Analysis of Reaction Rates

The reaction rate analysis recognizes the fast reactions among the thousands of reactions of the full mechanism. A reversible reaction i is identified as "fast" using its *normalized rate of reaction* $\overline{r_i(t)}$, which is defined as the absolute value of the ratio of the net rate r_i of the reaction (forward rate minus reverse rate) to the highest net rate $\mathrm{Max}(r_i(t))$ among all the reaction rates at a time-step t. Its value lies between 0 and 1 and takes into account the change of reactivity with time:

$$\overline{r_i(t)} = \left| \frac{r_i(t)}{\mathrm{Max}(r_i(t))} \right| \tag{1}$$

The group of fast reactions G_{fast} is selected by the following criterion using the rate-threshold ε_r:

If $\overline{r_i(t)} \geq \varepsilon_r$ *at each time-step, the reaction belongs to the group* G_{fast}.

The analysis is performed automatically by the post-treatment program CKRANA. It calculates the normalized rates over the entire autoignition delay time t_{ign} and selects the fast reactions according to values of ε_r fixed at 0.1, 0.01, or 0.001. These reactions must be kept in the reduced mechanism to maintain the dynamics of the overall rate of oxidation process. The slow reactions have a normalized rate lower than ε_r at one time-step at least. They are unimportant in the simulation of the dynamics of the autoignition process and should be discarded. However, some of the slow reactions are bottlenecks for the overall process because no competitive reaction offers a faster pathway. They must be recognized according to a different procedure discussed in the following section and cannot be discarded because of their character of rate-limiting reactions.

Sensitivity Analysis

The sensitivity analysis recognizes the rate-limiting reactions of the full mechanism. These reactions can be identified by searching for reactions with high sensitivity relative to a species or a group of species, which plays a leading part in the overall rate of reaction [8,33,34]. The radical OH is a main chain carrier in the oxidation and autoignition chemistry of hydrocarbons and was chosen as the target species. Its rate of production is closely linked to the overall reaction rate during a two-stage autoignition [35]. The program SENKIN calculates the first-order local sensitivity coefficient $S_{j,i}$ of species j and the temperature relative

to reaction i by

$$S_{j,i}(t) = \frac{\partial Z_j(t)}{\partial A_i} \tag{2}$$

$Z_j(t)$ is the mass fraction of species j at time t, and A_i is the pre-exponential factor of reaction i. The coefficients $S_{j,i}(t)$ are saved in the solution file as the elements of a very large matrix of $N_s + 1$ rows and N_r columns, where N_s and N_r are the numbers of species and reactions in the full mechanism, and an additional row takes into account the temperature variable. They assess the effect of an absolute infinitesimal change in A_i on the output quantity Z_j. The sensitivity coefficients as defined above cannot be compared to each other because the parameters A_i for reactions of different orders have different units and the values of Z_j and A_i span many orders of magnitude. The log-normalized sensitivity coefficients $\overline{S_{j,i}(t)}$ based on relative infinitesimal changes are preferred:

$$\overline{S_{j,i}(t)} = \frac{\partial Z_j(t)/Z_j(t)}{\partial A_i/A_i} = \frac{\partial \ln Z_j(t)}{\partial \ln A_i} = \frac{A_i}{Z_j(t)} S_{j,i}(t) \tag{3}$$

The posttreatment program CKSENS calculates the log-normalized sensitivity coefficient $\overline{S_{\mathrm{OH},i}(t^*)}$ relative to OH, at a selected time t^* and ranks all reactions in decreasing order of sensitivity coefficients according to the index k. The reactions are ordered from high sensitivity to low sensitivity. It is necessary to specify a threshold where insensitive reactions can be neglected. As the values of $\overline{S_{\mathrm{OH},k}(t^*)}$ cover many order of magnitude, the setting of a reasonable threshold is not an easy task. It is more convenient to define a number of rate-limiting reactions N_{r-1}. Its value can be obtained by plotting $\log \overline{S_{\mathrm{OH},k}(t^*)} - \log \overline{S_{\mathrm{OH},k+1}(t^*)}$ versus the rank k. Figure 1 shows an example of this plot. The prominent maximum observed in this example at a particular rank k corresponds to a large gap between two successive values of $\overline{S_{\mathrm{OH},k}(t^*)}$. This gap indicates a clear delineation between sensitive reactions and insensitive reactions and is of a great help in defining a sensible value of k as a *cutting rank* k_{cut}. It is an indicator of the size order of N_{r-1}. The optimal value of N_{r-1} is deduced by testing mechanisms, with N_{r-1} changed incrementally in steps of 100. The resulting mechanisms are tested by comparison to the fully detailed model, and the optimal mechanism (and N_{r-1}) is deduced. So, *the group of rate-limiting reactions* G_{r-1} is selected by the following criterion based on the threshold N_{r-1}:

If the rank k of reaction is like $k \leq N_{r-l}$, *the reaction belongs to the group* G_{r-l}.

The calculation of the sensitivity coefficients expends large computational resources. A sensitivity calculation using Aurora in CHEMKIN 4.0 with the isooctane mechanism of 858 species and 3603 reactions takes 70 h of computer time on an Intel Zeon 2.2 GHz processor. A subsequent calculation for a fuel-rich case with a 1.2 equivalence ratio was not completed in 200 h, which was the maximum time limit allowed for runs on this machine. Also the solution files created by sensitivity runs can be very large. A computer run of the SENKIN code of CHEMKIN-II using a methane mechanism of 38 species and 190 reactions produces a solution file of 15 GB. However, this problem of large solution files has been addressed in later version of CHEMKIN (version 4.0).

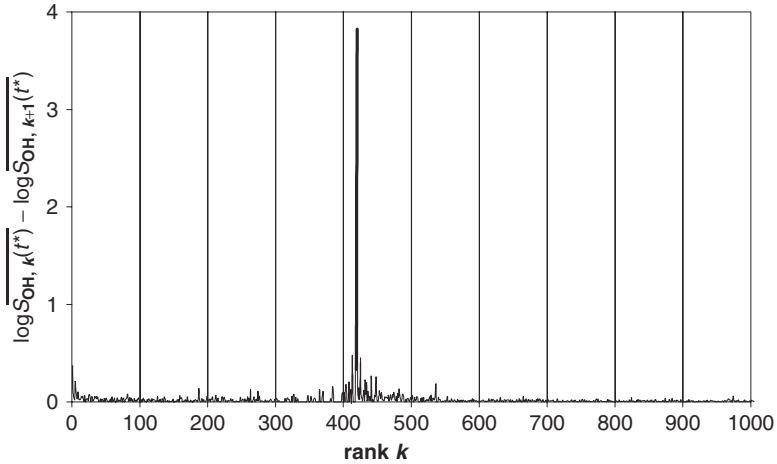

Figure 1 Plot of $\log\overline{S_{\mathrm{OH},k}(t^*)} - \log\overline{S_{\mathrm{OH},k+1}(t^*)}$ versus rank k obtained for Curran and coworker's mechanism of isooctane in the following input simulation conditions: mixture iso-$C_8H_{18}/O_2/N_2 = 0.0165/0.2065/0.7770$ (in mole fractions), 13.3 bar, 702 K. In this case the value of k_{cut} is 420.

Since SENKIN in the CHEMKIN-II suite of codes was used in the present calculations, an alternative strategy had to be undertaken to avoid the expenditure of large computer resources. Several tests indicated that identification of the rate-limiting reactions can be performed at a single time t^*, and this identification is relatively insensitive to the value of the time t^*. For this local sensitivity calculation, it is important to choose a time where the characteristic autoignition chemistry is very active. Reaction path analysis shows that reactions characteristic of autoignition chemistry are very active at a time t^* equal to half of the autoignition delay time. Therefore, this time was chosen to compute these local sensitivities. The calculation procedure was as follows: A SENKIN calculation without sensitivity analysis was performed from time zero to autoignition and the solution file was saved. This calculation was very fast. Then the SENKIN calculation was restarted at a time slightly below t^* using the previously computed solution and sensitivity analysis turned on. This procedure saved computing time and memory storage because the calculation of the sensitivity matrix was limited to a few time-steps until the time t^* was reached. The solution file from the second SENKIN run was used for identification of a group of rate-limiting reactions. We have tested the validity of this procedure on a mechanism of hydrogen. We have compared the values of local sensitivity coefficients obtained with this procedure at selected times when the autoignition chemistry is very active. Then we compared the results to the global sensitivity results computed from a sensitivity analysis calculation starting at time zero. The absolute values of the sensitivity coefficients were not exactly the same in the two cases. However, the relative rankings were exactly the same. As the selection of the group of rate-limiting reactions is based on the ranking of sensitivity coefficients and not on the individual values of sensitivity coefficients, this shows the procedure is valid.

Selection of Redundant Reactions

Figure 2 illustrates the principle of selection of redundant reactions by coupling the analysis of reaction rates with the analysis of sensitivity. The reactions of the reduced mechanism are the union of the fast reactions G_{fast} and the rate-limiting reactions $G_{\text{r}-1}$. The discarded redundant reactions are slow and non–rate-limiting together.

The program CKRANA builds the reduced mechanism automatically. It is written by selecting the species that appear both in fast and in rate-limiting slow reactions and adding the corresponding reactions and kinetic parameters.

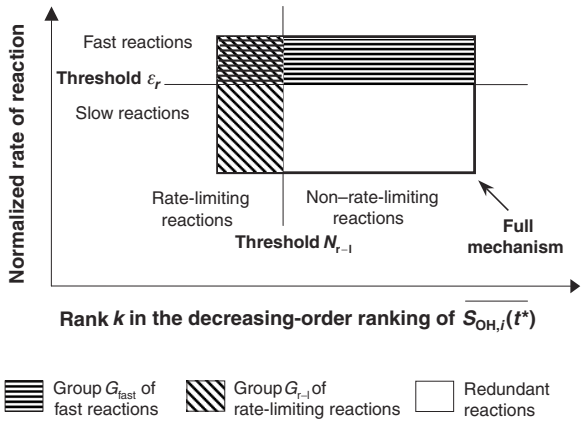

Figure 2 Principle of redundant reaction selection and mechanism reduction.

THE THRESHOLDS, SIZE, AND EFFICIENCY OF REDUCED MECHANISMS

The size and the efficiency of a reduced mechanism (RM) depends on the threshold for the fast reactions ε_r and for the rate-limiting reactions $N_{\text{r}-1}$. The joint analyses of reaction rates and sensitivities are performed on the results of an autoignition simulation. As the oxidation and autoignition chemistry depends strongly upon the temperature at which it occurs, the input temperature or *analysis temperature* T_{ana} of the simulation is also a factor that influences the size and efficiency of the final RM. The values of ε_r, $N_{\text{r}-1}$, and T_{ana} were successively changed keeping the two other parameters constant, and the ignition delay times predicted by the reduced mechanisms (RMs) were compared with those predicted by the full mechanism (FM). A discrepancy between the values of ignition delay times predicted by the FM and the RM can be high but not detectable from the graph if these values are small compared to the scale of the graph. To have a reliable criterion of efficiency, we define the average error E on the ignition delay time:

$$E = \frac{\sum_{1}^{N} \frac{t_{\text{ign}}(\text{RM}) - t_{\text{ign}}(\text{FM})}{t_{\text{ign}}(\text{FM})}}{N}$$

where t_{ign}(RM) is the ignition delay time predicted by the RM, t_{ign}(FM) is the ignition delay time predicted by the FM, and N is the number of simulations performed at different temperatures.

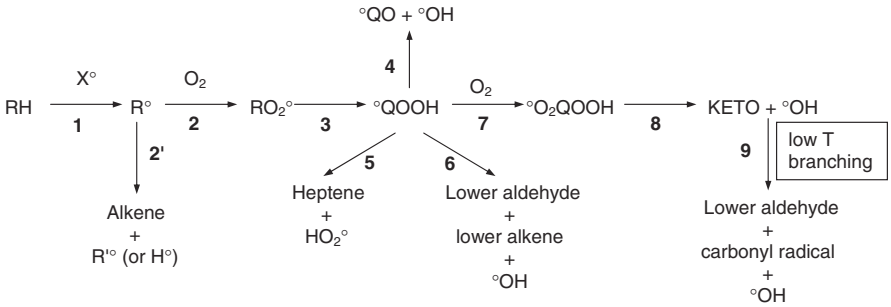

Figure 3 Reaction scheme of the primary oxidation mechanism of *n*-heptane involving C_7 species. RH is for *n*-heptane, R° for heptyl radicals, Q for C_7H_{14} structures, Q′ for C_7H_{13} structures, QO for O-heterocycles, KETO for ketohydroperoxides or aldo-hydroperoxides and X° for °OH, CH_3°, CH_3O°, CH_3O_2°, HO2°, or H°.

Full Test Mechanism

The mechanism of oxidation of *n*-heptane developed by Curran et al. [4] was chosen as fully detailed test mechanism. *n*-Heptane is the first reference fuel for octane rating for spark-ignited engines and its cetane number is close to that of diesel fuels. A better understanding of its oxidation kinetics is useful to predict autoignition and pollutant formation in engines. Curran and coworkers' mechanism describes the oxidation chemistry of C_0–C_7 species in the low- and high-temperature ranges and contains 545 species in 2446 reactions. Figure 3 shows the main types of reactions of C_7 species of the primary oxidation mechanism of *n*-heptane. The *n*-heptane mechanism has been validated in a large range of conditions of temperature (650–1550 K), of pressure (2.2–42 bar), of equivalence ratio (0.5–2.0), and of dilution (70%–98%). The experimental data used for validation have been obtained in a variable pressure flow reactor (VPFR) [36], a rapid compression machine (RCM) [37,38], a jet-stirred reactor (JSR) [39,40], and a shock tube [41–43]. Typical data were the ignition delay times at low and high temperatures (RCM and shock tube studies) and the species concentration profiles (VPFR and JSR studies). The validated detailed mechanism allowed assessment of the efficiency of RMs in the same large range of parametric conditions and for various types of data.

Influence of the Threshold ε_r

The influence of ε_r was studied for calculated ignition delay times in the parametric conditions of the RCM [38]: 650–900 K, 3.3–4.5 bar, $\phi = 1.0$, and a dilution of 78%. RMs were generated for the state of a mixture compressed in the RCM at 3.7 bar and $T_{ana} = 710$ K, a temperature characteristic of the low-temperature range.

Figure 4 illustrates the influence of the threshold ε_r on the efficiency of the RMs. Four values of

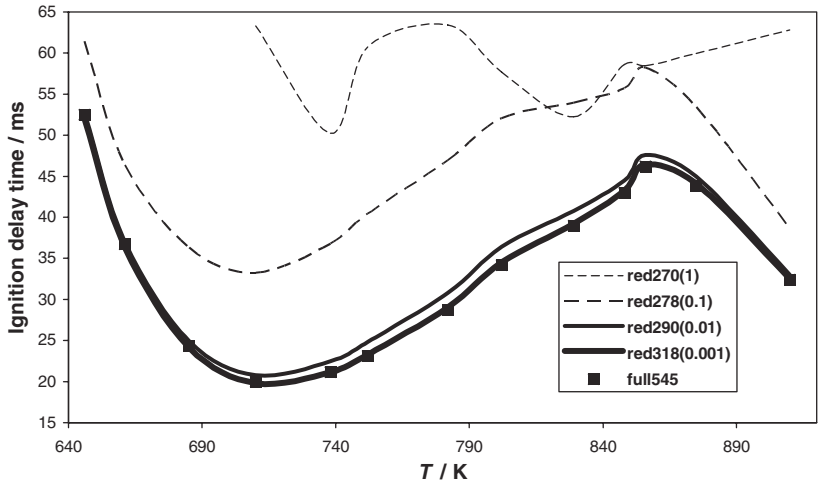

Figure 4 Ignition delay times of *n*-heptane/O_2/diluent mixtures versus temperature calculated predicted with the FM and the RMs with $\varepsilon_r = 1$–0.001 and $N_{r-1} = 500$. The number of species is given in each case. Conditions of the RCM study in [38]: 3.3–4.5 bar, $\phi = 1.0$, dilution with 78% of air.

ε_r (1, 0.1, 0.01, or 0.001) were used to generate four RMs: red270, red278, red290, and red318 containing 270, 278, 290, and 318 species and 500, 526, 604, and 788 reactions, respectively. The threshold N_{r-1} was kept at 500. As the numbers of species and reactions in the RM increase when ε_r decreases, the agreement between the results of the RM and the full mechanism (FM) is better when ε_r is smaller. The RM red318 produces results fully in agreement with the FM as confirmed by the low value of the average error: $E = 0.7\%$. The RM red290 can be considered as a suitable compromise between the level of reduction and the efficiency: the predictions are in agreement with the FM with $E = 3.9\%$. The RM red278 reproduces the shape of the curve well, but the delay times are 42.9% too long on average. The RM red270 failed completely. Obviously, a reduction process cannot be based on a rate-limiting reaction criterion only.

Table I presents the species, ranked from C_2 to C_6, that are suppressed from the FM when ε_r is changed. Eighteen species are suppressed when ε_r is changed from 0.001 (red318) to 0.01 (red290). Most of them are C_4 species: five are species pertaining to the oxidation chemistry of *sec*-butyl radical and two are radicals formed from but-2-ene (c4h8oh-2, o2c4h8oh-2). Twelve species are suppressed when ε_r is changed from 0.01 (red290) to 0.1 (red278). Again, most of them are C_4 species: but-2-ene,*sec*-butyl, *sec*-butylperoxy, 2-hydroperoxybut-3-yl (c4h8ooh2-3) radicals, and but-2-ol-1-yl and but-2-ol-1-peroxy radicals formed from but-1-ene. The corresponding change of E from 42.9% (red290) to 3.9% (red278) shows that the oxidation chemistry of butenes and the *sec*-butyl radical takes a major part in the overall oxidation rate of *n*-heptane. The *sec*-butyl radical is formed by the addition of a hydrogen atom to the but-1-ene issued from the decomposition of 3-hydroperoxyhept-5-yl, heptenyl, and hept-3-yl radicals. But-2-ene is formed either by the reaction of butenyl radical with HO_2 and with ethanal or by the decomposition of c4h8ooh2-3. The latter results from an isomerization of the *sec*-butylperoxy radical.

Influence of the Threshold N_{r-l}

As for the threshold ε_r, the influence of the threshold N_{r-1} on calculated ignition delay times was studied under the experimental conditions of the RCM [38]. The analyses were performed with the set of simulation conditions used to examine the influence of ε_r. Six values of N_{r-1} (0, 100, 200, 300, 400, and 500) generated six RMs with 185, 194, 213, 236, 263, and 290 species and 384, 396, 435, 497, 570, and 604 reactions, respectively. The value of ε_r was kept equal to 0.01.

Figure 5 illustrates the influence of N_{r-1} on the efficiency of the RMs. The agreement between the results of the RM and those of the FM is better when N_{r-1} is increased. Adding rate-limiting reactions to the group of fast reactions lowers E from 28% to 3%. The discrepancies are higher in the region 700–860 K of the negative temperature coefficient (NTC) and in the range 860–900 K with the maximum discrepancy at the end of the NTC region.

When N_{r-1} is decreased from 200 (red185) to 0 (red213), most of the suppressed reactions are the

Table I Species Suppressed in the FM with ε_r Changing from 0.001 to 0.01 Then from 0.01 to 0.1

C_2	C_3	C_4	C_5	C_6
Species of the RM red318 ($\varepsilon_r = 0.001$) Suppressed in the RM red290 ($\varepsilon_r = 0.01$)				
c2h	c3h3	c4h8ooh2-4	ic5h9	c6h12-3
c2h3o1-2	c3h8	c4h8ooh2-3o2	bc5h10	
sc2h4oh	c3h4-a	c4h8ooh2-4o2	cc5h10	
	c3h4-p	nc4ket23	bc5h11	
	ic3h7o	nc4ket24	dc5h11	
	ch3chco	c4h8oh-2	c2h5coc2h5	
	ch2cch2oh	o2c4h8oh-2	c3h6coch3-2	
		ic4h8		
		c4h10		
		c3h8coch3-2		
Species of the RM red290 ($\varepsilon_r = 0.01$) Suppressed in the RM red278 ($\varepsilon_r = 0.1$)				
o2c2h4oh	ic3h7	sc4h9		nc4h9coch3
pc2h4oh	ic3h7o2	sc4h9o2		
	ch3coch3	c4h8ooh2-3		
		c4h8-2		
		c4h8oh-1		
		o2c4h8oh-1		

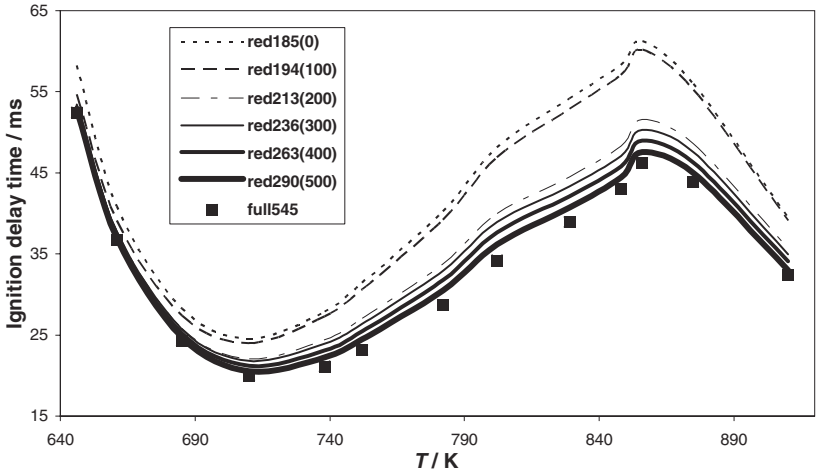

Figure 5 Ignition delay times of *n*-heptane/O_2/diluent mixtures versus temperature calculated with the FM and six RMs with $N_{r-1} = 0$–500 and $\varepsilon_r = 0.01$. The number of species is given in each case. Conditions of the RCM study in [38]: 3.3–4.5 bar, $\phi = 1.0$, dilution = 78%.

decomposition of °QOOH to an O-heterocycle and OH (type 4), the addition of O_2 to °QOOH (type 7), the isomerization of °O_2QOOH to ketohydroperoxides (type 8), and ketohydroperoxide decomposition (type 9) (see Fig. 3). The results of the brute-force sensitivity analysis of rate parameters to ignition delay time made by Curran et al. at 800 and 910 K show that reaction types 4–9 are among the most sensitive [4]. Reaction types 4–6 have positive sensitivity coefficients, which indicate that an increase in their rate constants decreases the overall reactivity, whereas reactions types 7–9 have negative sensitivity coefficients. There is thus a strong competition between the chain-branching reaction paths 7–9 leading to decomposition of ketohydroperoxide and the chain-propagation paths 4–6 of °QOOH radical decomposition, in the NTC region and up to 910 K. The balance between branching and propagation paths is delicate, and the suppression of reactions 4, 7, 8, and 9, when N_{r-1} is decreased from 200 to 0, has a great impact on the overall oxidation rate and thus on ignition delay times. These considerations explain the serious deterioration of the predictions. However, even when N_{r-1} is 0 (i.e., no rate-limiting slow reaction is added to the group of fast reactions), the shape of the curve is retained. By contrast to a reduction process based only on the criterion of the rate-limiting steps, a reduction process based only on the analysis of reaction rates generates quite a satisfactory mechanism.

Influence of the Analysis Temperature T_{ana}

The influence of the input temperature T_{ana} of the basic simulation on calculated ignition delay times was studied in the conditions of the shock tube study in [41]: high-temperature range 1270–1560 K, 2.2 bar, $\phi = 1.0$, 70% of dilution in argon. The RMs were generated in the high-temperature range for the state of a mixture after the passage of a shock wave at $T_{ana} = 1270$ K. The RM red227 with 604 reactions was generated using $\varepsilon_r = 0.01$ and $N_{r-1} = 500$.

In Fig. 6, the efficiency of the RM red227 is compared to those of the RMs red290 and red318, which were generated with the conditions $T_{ana} = 710$ K, $N_{r-1} = 500$, and $\varepsilon_r = 0.01$ and 0.001. Figure 6 also shows how the efficiency of the RM changes according to whether T_{ana} belongs to the low-temperature

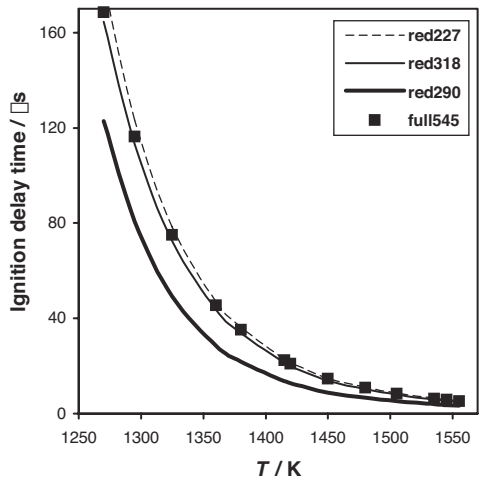

Figure 6 Ignition delay times of *n*-heptane/O_2/diluent mixtures versus temperature calculated with the FM and three RMs : red227 ($N_{r-1} = 500$, $\varepsilon_{r-1} = 0.01$, $T_{ana} = 1270$ K), red290 ($N_{r-1} = 500$, $\varepsilon_r = 0.01$, $T_{ana} = 710$ K) and red318 ($N_{r-1} = 500$, $\varepsilon_r = 0.001$, $T_{ana} = 710$ K). Conditions of the shock tube study in [41]: 2.2 bar, $\phi = 1.0$, dilution with 70% of Ar.

range, here 710 K, or to the high-temperature range, here 1270 K. The predictions of the RM red290 are poor with $E = 36.4\%$, whereas the predictions of the RM red227 are very good with $E = 2.7\%$. The reduced accuracy of the RM red290 compared to the RM red227 results from the suppression of key species found in RM red290, inducing a shortening of the delay times. Among them were the radicals CH, C_2H, allyl, and propargyl, known as essential in the high-temperature chemistry. Although the RM red290 has a larger number of species than RM red277, it is less efficient because the analysis temperature $T_{ana} = 710$ K does not belong to the temperature range of the simulated delay times. However, if the level of reduction is lowered by putting $\varepsilon_r = 0.001$, the corresponding RM red318 reproduces correctly the ignition delay times at high temperatures with $E = 1.7\%$. Obviously, an RM generated with an analysis temperature in the low-temperature range is able to predict autoignition in the high-temperature range, but an RM generated with an analysis temperature in the high range is not able to predict autoignition in the low-temperature range. In fact, all the C_7 $^\circ O_2QOOH$ and KETO species of Table II and many similar C_6 and C_5 species have been suppressed in the RM red227. At high temperatures, the reactions 7–9 (Fig. 3), in which these species are involved, are slow but non–rate-limiting and can be suppressed. At low temperatures, they are rate-limiting and their suppression would shut off the low-temperature branching and produce a too low rate of oxidation to promote autoignition.

The reduction with an analysis temperature in the high-temperature range leads to a higher level of reduction than with an analysis temperature belonging to the low-temperature range: 227 species and 540 reactions in the first case against 290 species and 604 reactions in the second case. At high temperature, the $^\circ$QOOH radicals decompose more readily through reactions 4–6 instead of adding O_2 through reactions 7 (see Fig. 3). The contributions of reactions 7–9 to the overall rate of the oxidation process become negligible because the decomposition channels are more sensitive to the temperature than the addition reactions 7 which have zero activation energy. Moreover, the equilibria $O_2 + QOOH = O_2QOOH$ shift to the reverse direction in the high-temperature range. The reactions 5 are fast, and the reactions 4 and 6 are slow and rate limiting. They are both unaffected by the reduction process. On the other hand, the reactions 7–9 are slow but non–rate-limiting and can be discarded. The C_7 species $^\circ O_2QOOH$ and KETO and some products of decomposition of KETO are suppressed (see Table II) because they are redundant species in the high-temperature range, whereas they are essential in the low-temperature range. As the symbols $^\circ O_2QOOH$ and KETO stand for multiple isomeric structures, their suppression leads to a drastic reduction in the number of species and reactions. Table II shows that 18 C_7, 7 C_6, and 6 C_5 similar species of the types $^\circ O_2QOOH$ and KETO are suppressed in the RM red227.

VALIDATION OF THE REDUCED MECHANISMS

Reduced Mechanism for *n*-Heptane

Table III lists the sizes and parameters of the RMs for *n*-heptane. It also contains the number of rate-determining fast reactions, the number of rate-limiting

Table II Key Species of the RM red290 Suppressed in the RM red227

KETO	nc7ket12 nc7ket13 nc7ket14 nc7ket15 nc7ket21 nc7ket23 nc7ket24 nc7ket25 nc7ket26 nc7ket31 nc7ket32 nc7ket34 nc7ket35 nc7ket36 nc7ket37 nc7ket41 nc7ket42 nc7ket43	nc6ket12 nc6ket13 nc6ket14 nc6ket21 nc6ket23 nc6ket24 nc6ket25	nc5ket13 nc5ket14 nc5ket15 nc5ket21 nc5ket24 nc5ket25
$^\circ O_2QOOH$	c7h14ooh1-2o2 c7h14ooh1-3o2 c7h14ooh1-4o2 c7h14ooh1-5o2 c7h14ooh2-1o2 c7h14ooh2-3o2 c7h14ooh2-4o2 c7h14ooh2-5o2 c7h14ooh2-6o2 c7h14ooh3-1o2 c7h14ooh3-2o2 c7h14ooh3-4o2 c7h14ooh3-5o2 c7h14ooh3-6o2 c7h14ooh3-7o2 c7h14ooh4-1o2 c7h14ooh4-2o2 c7h14ooh4-3o2	c6h12ooh1-2o2 c6h12ooh1-3o2 c6h12ooh1-4o2 c6h12ooh2-1o2 c6h12ooh2-3o2 c6h12ooh2-4o2 c6h12ooh2-5o2	c5h10ooh1-3o2 c5h10ooh1-4o2 c5h10ooh1-5o2 c5h10ooh2-1o2 c5h10ooh2-4o2 c5h10ooh2-5o2
Decomposition products of KETO	nc5h11cho nc5h11co nc4h9cho nc4h9co ch2ch2coch3 c3h6coch3-1 nc4h9coch2 c2h5coc2h4p c3h6coc2h5-1 nc3h7coc2h4p		

slow reactions, and the gain in CPU time for the simulation of autoignition delay times. The computations were carried out on an IBM Power 4 using 1 processor. The RMs were tested in a large range of conditions (600–1500 K, 3–42 bar, ϕ = .5–2.0, 70%–98% of dilution) and for different types of data (cool flame delay times, ignition delay times, species mole fraction profiles). Simulations of PSR data were performed using the module AURORA of the package CHEMKIN III [44].

Figure 4 shows a comparison between the ignition delay times predicted by the FM and the three RMs red278, red290, and red318 over a range of low temperatures and rather low pressures. The RM red290 offers the best compromise between the level of reduction and the efficiency with $E = 3.9\%$.

Figures 7a–c show the comparison in a larger range of temperature, at a higher pressure, and for three equivalence ratios. The predictions of red318 are in complete agreement with the FM, the average error E lying between 0.7% and 1.1%. The predictions of the RM red278 are worse below 1000 K for the lean mixture and in the NTC region for the stoichiometric and rich mixtures, with E between 19.5% and 56.3%. The RM red290 offers the best compromise, with E equal to 5.8%, 4.5%, and 4.6% for $\phi = 0.5$, 1.0, and 2.0, respectively.

Figures 8a, 8b, and 7b present the ignition delay times predicted by the FM and the RMs red278, red290, and red318 in the temperature range 650–1340 K and at 6.5, 13.5, and 42 bar, respectively. The RM red318 gives the best agreement, with E between 0.8% and 1.3%. The predictions of the RM red278 are worse, with E between 21.2% and 43.4%. The RM red290 is the best compromise, with E equal to 8.5% at 6.5 bar, 4.5% at 13.5 bar, and 4.2% at 42 bar.

The RMs red278, red290, and red318 were also tested at the higher temperatures of the shock tube study in [41] (see Fig. 9). Only the RM red318 gives good results, with $E = 4.9\%$. The RM red227 generated at $T_{\text{ana}} = 1270$ is more efficient, with $E = 2.7\%$, although its number of species is 29% lower than that of the RM red318. Attempts to reach a higher level of reduction at temperatures above 1290 K as in Coats

Table III Principal Features of *n*-Heptane Mechanisms

Mechanism	full545	red318	red290	red278	red227
Number of species	545	318	290	278	227
Number of reactions	2446	788	604	526	540
ε_r	–	0.001	0.01	0.1	0.01
N_{r-1}	–	500	500	500	500
T_{ana}	–	710	710	710	1270
Number of fast reactions	–	667	334	109	215
Number of rate-limiting slow reactions	–	121	270	417	325
Speedup factor	–	4.2[a]	5.9[a]	7.1[a]	50[b]

[a] For the 13 autoignition simulations corresponding to Fig. 4.
[b] For the 13 autoignition simulations corresponding to Fig. 9.

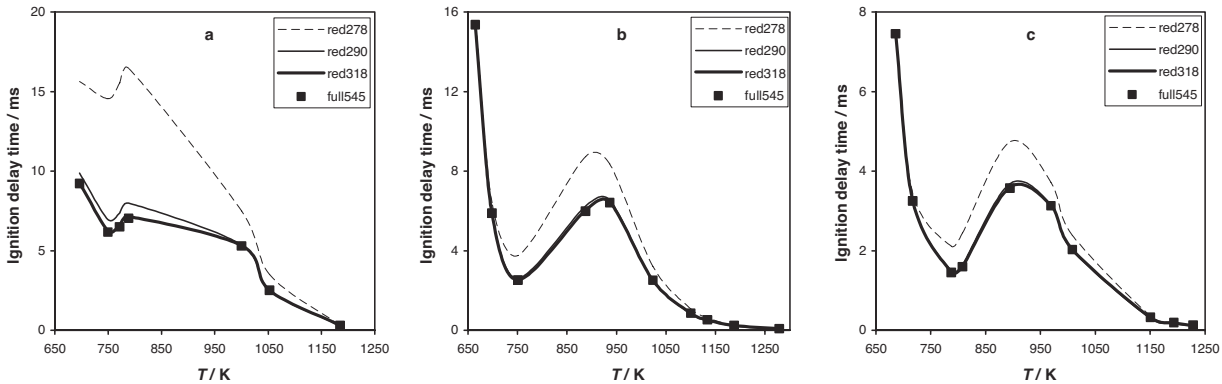

Figure 7 Ignition delay times of *n*-heptane/O_2/diluent mixtures versus temperature calculated with the FM and three RMs. The number of species is given in each case. Conditions of the shock tube study in [43]: 13.5 bar, dilution with 78% of Ar, (a) $\phi = 0.5$, (b) $\phi = 1.0$, and (c) $\phi = 2.0$.

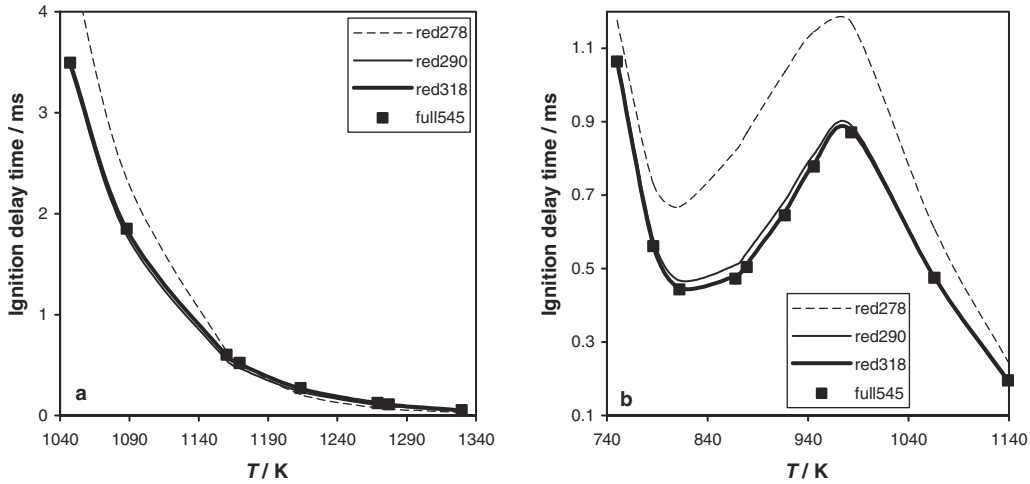

Figure 8 Ignition delay times of *n*-heptane/O_2/diluent mixtures versus temperature calculated with the FM and three RMs. The number of species is given in each case. Conditions of the shock tube study in [43]: $\phi = 1.0$, dilution with 78% of Ar, (a) 6.5 bar and (b) 42.0 bar.

and Williams' shock tube study in [42] have shown that the limit in reduction in the high-temperature range is reached with the RM red227.

Figure 10 exhibits the comparison between the predictions of the FM and those of the RMs red278, red290, and red318 for mole fraction profiles of oxidation products in the conditions of the JSR study in [39,40]. An average error on profile is calculated similarly to the average error on ignition delay time, taking into account each temperature of the profile. Although the gap between the predictions of the RM red278 and the FM looks small, the average error lies between 13.3% for CO_2 and 44.2% for hept-3-ene. The predictions of the RMs red318 and red290 are better, with E between 2.1% and 3.5% depending on the product. The RM red290 offers the best compromise between the level of reduction and the ability to reproduce the results of the FM.

The speedup factor for the selected RMs varies from 4.2 to 50: it increases nonlinearly with the number of species and cannot be increased more than 50 (see Table III). When ε_r is varied from 0.01 to 0.1, the CPU time reduction increases slightly but the quality of the predictions is strongly damaged. In most of the parametric conditions, the value $\varepsilon_r = 0.01$ is the best choice: the corresponding RM red290 gives the best compromise between the level of reduction and the ability to reproduce the results of the FM.

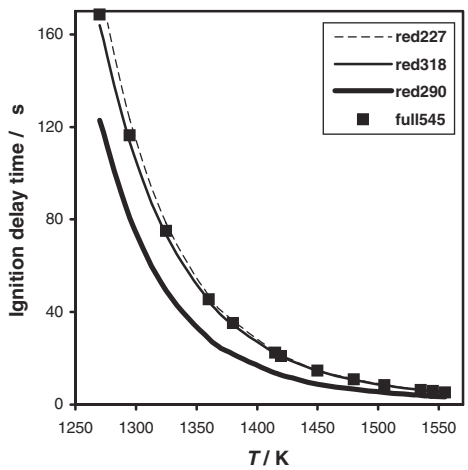

Figure 9 Ignition delay times of *n*-heptane/O_2/diluent mixtures versus temperature calculated with the FM and three RMs. The number of species is given in each case. Conditions of the shock tube study in [41]: 2.2 bar, $\phi = 1.0$, dilution with 70% of Ar.

Reduced Mechanism for Isooctane

Isooctane is the second reference fuel for octane rating in spark-ignition engines. It is used as neat fuel and as a component of primary reference fuel blends in current investigations of HCCI engines. A better understanding of its oxidation kinetics would be very valuable for predicting autoignition and pollutant emissions during the combustion process. Curran and coworkers' mechanism of isooctane [5] describes the oxidation chemistry of C_0 to C_8 species in the low- and high-temperature ranges and contains 858 species and 3606 reactions. It was validated in a wide range of

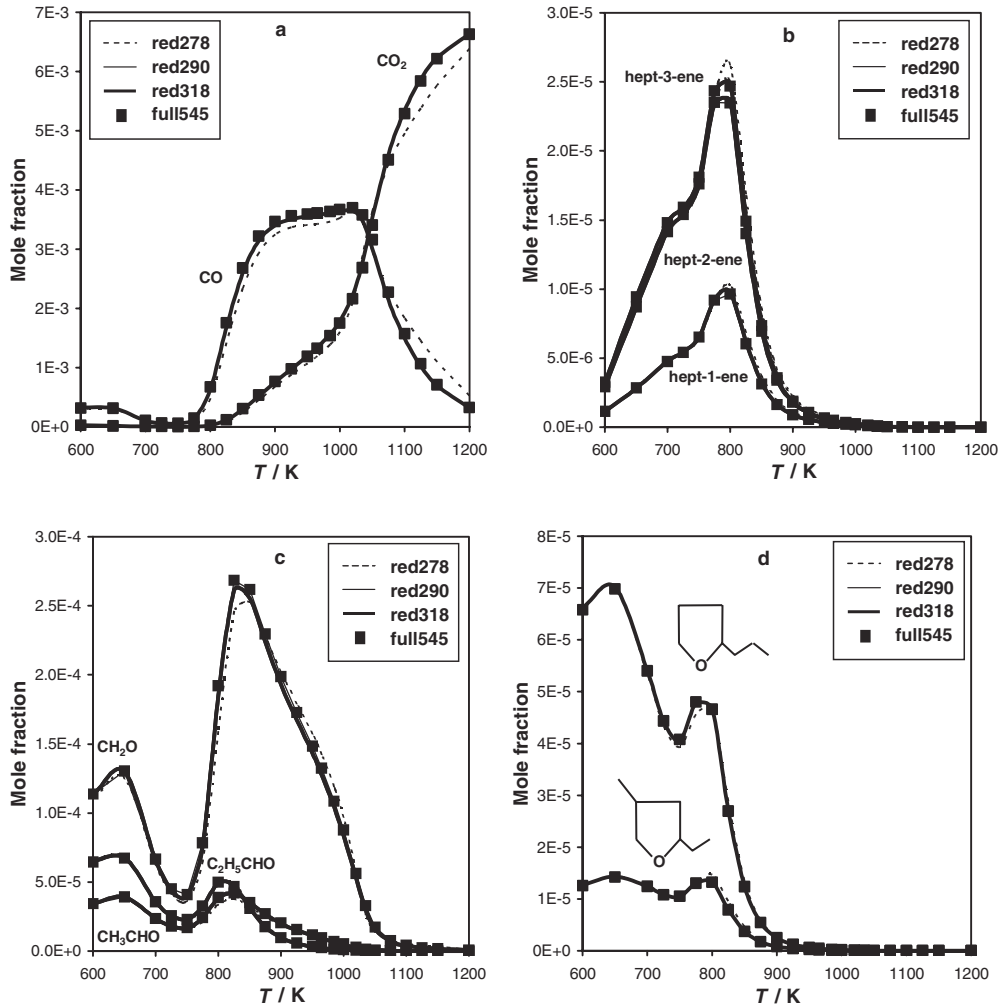

Figure 10 Mole fraction-temperature profiles of some oxidation products calculated with the FM and three RMs. The number of species is given in each case. Conditions of the JSR study in [39,40]: 9.9 bar, residence time = 1 s, $\phi = 1.0$, dilution with 98% of Ar, (a) CO and CO_2, (b) heptenes, (c) aldehydes, and (d) O-heterocycles.

conditions (550–1700 K, 1–45 bar, 0.3–1.5 for ϕ, 70%–90% dilution) against ignition delay times obtained in shock tubes and species concentrations measured in a JSR, VPFRs, and in a CFR engine. This mechanism is also a valuable test mechanism for the reduction technique because the efficiency of the RMs can be measured in a large range of parametric conditions and for various types of data.

Table IV presents the main features of the RMs. The optimal value of N_{r-1} was found equal to 500 and three values of ε_r, 0.1, 0.01, and 0.001, generated the RMs red300, red325, and red392, respectively. The analysis temperature was taken equal to 702 K in order to produce RMs valid in the low-temperature and high-temperature ranges. The RMs were tested in the broad range of conditions (690–1300 K, 13–45 bar, $\phi = .5$–2.0, 78% dilution in N_2) corresponding to the shock tube study in [45].

Figures 11a–c present the comparison between the ignition delay times predicted by the FM and the RMs for three equivalence ratio: $\phi = 0.5$, 1.0, and 2.0, respectively. The predictions of the RM red392 are in perfect agreement with those of the FM: E varies from 0.2% to 0.7%. Although they appear quite good in the figures, the predictions of the RM red300 are in high disagreement with those of the FM: E varies from 10.8% to 39.2%, the largest discrepancies being above 1000 K for the lowest ignition delay times. The RM red325 is the best compromise with low values of E equal to 0.8%, 2.0%, and 3.8% for $\phi = 0.5$, 1.0, and 2.0, respectively.

Figures 12a–c depict the comparison between the ignition delay times predicted by the FM and the RMs for three pressures: 13, 35, and 45 bar, respectively. The RM red325 corresponds again to the best compromise, with $E = 3.6\%$, 3.1%, and 2.6% at 13, 35, and 45 bar,

Table IV Principal Features of Isooctane Mechanisms

Mechanism	full545	red392	red325	red300
Number of species	858	392	325	300
Number of reactions	3606	1039	731	550
ε_r	–	0.001	0.01	0.1
N_{r-1}	–	500	500	500
T_{ana}	–	702	702	702
Speedup factor	–	7.7[a]	16.7[a]	33.3[a]

[a] For the 11 autoignition simulations corresponding to Fig. 11b.

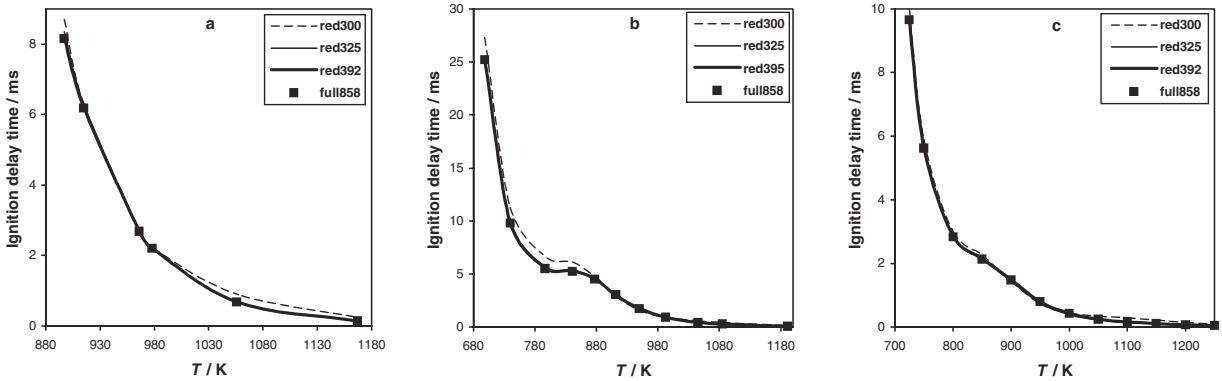

Figure 11 Ignition delay times of isooctane/O_2/diluent mixtures versus temperature calculated with the FM and three reduced mechanisms. The number of species is given in each case. Conditions of the shock tube study in [45]: 40 bar, dilution with 78% of N_2, (a) $\phi = 0.5$, (b) $\phi = 1.0$, and (c) $\phi = 2.0$.

respectively. The same conclusion was drawn when the RMs were tested on species and temperature rise profiles in the conditions of the VPFR study in [36] (Fig. 13).

The speedup factor increased nonlinearly from 7.7 to 33.3 when the number of species decreased from 392 to 300 (Table IV). When ε_r was increased from 0.01 to 0.1, the number of species decreased slightly from 325

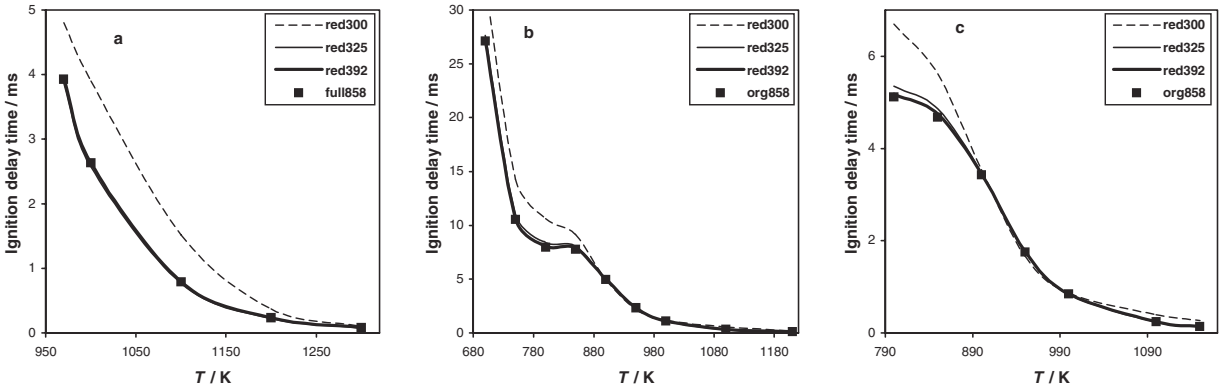

Figure 12 Ignition delay times of isooctane/O_2/diluent mixtures versus temperature calculated with the FM and three RMs. The number of species is given in each case. Conditions of the shock tube study in [38]: $\phi = 1.0$, dilution with 78% of N_2, (a) $\phi = 13$ bar, (b) 35 bar, and (c) 45 bar.

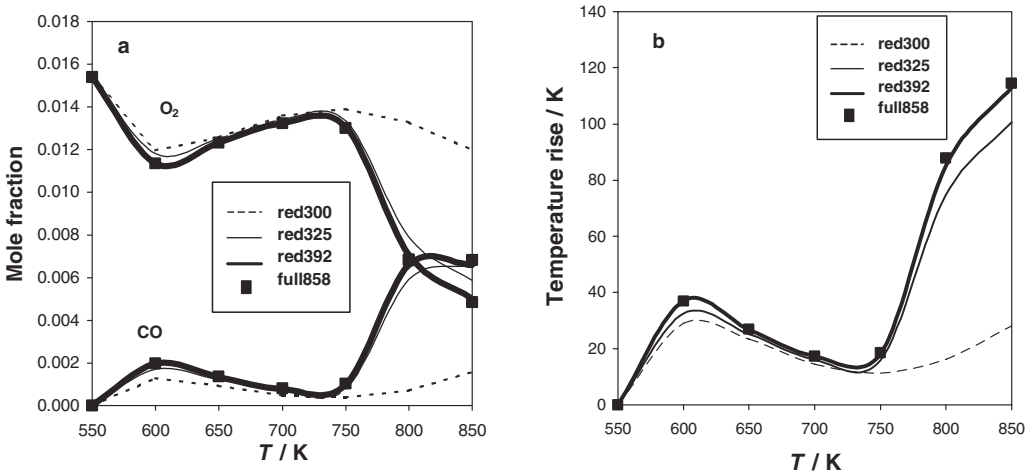

Figure 13 Mole fraction-temperature profiles of some oxidation products calculated by the FM and three RMs. The number of species is given in each case. Conditions of the VPFR study in [36]: 12.5 bar, residence time = 1.8 s, $\phi = 1.0$, dilution with 99% of N_2, (a) CO and O_2 and (b) temperature rise.

to 300, but the quality of predictions was significantly degraded. The RM red325 is the best compromise.

CONCLUSION

For the first time, a new reduction technique of kinetic mechanisms of autoignition based on joint analyses of reaction rates and sensitivities has been developed. The reaction rate analysis divides the entire set of reactions into fast and slow reactions by normalizing the rates and defining a rate threshold ε_r. The sensitivity analysis divides the entire set of reactions into a group of rate-limiting reactions and a group of non–rate-limiting reactions; a rate-limiting reaction is identified as a reaction exhibiting a high-local sensitivity coefficient with respect to the radical OH. The criterion of distinction between the non–rate-limiting and rate-limiting reactions is based on the threshold N_{r-1}, which is the number of reactions in the group of rate-limiting reactions. The optimal values of the thresholds ε_r and N_{r-1} are obtained by a try and error procedure and are specific of the considered full mechanism. They are determined from analyses performed on an arbitrarily chosen simulation of ignition. For computing technical reasons, sensitivity coefficients at half of ignition delay time are only considered.

The reduced mechanism consists of the union of the set of fast reactions and rate-limiting reactions. Reactions that are not "fast reactions" or "rate-limiting reactions" are redundant and not included in the reduced mechanism. Species included only in these redundant reactions are called "redundant species" and are eliminated from the detailed mechanism.

The reduction procedure is carried out by two computer programs: (i) CKSENS performs the sensitivity analysis and (ii) CKRANA performs the analysis of reaction rates and builds the RM. CKSENS and CKRANA are compatible with the software package CHEMKIN-II.

The technique is fast and easy to apply. A thorough knowledge of the detailed mechanism is not required, and only two thresholds of reduction have to be chosen. An RM is generated in less than 5 min. The longest operation is the finding of the cutting rank to deduce the optimal number of rate-limiting reactions. However, the procedure could be automated.

The reduced mechanisms obtained by our technique are efficient. For Curran's n-heptane mechanism, the optimal RM corresponds to a speedup factor of 5.9 and a reduction of 47% of the number of species, whereas for Curran's isooctane mechanism it corresponds to a speedup factor of 16.7 and a reduction of 62% of the number of species. The size of the RM and its ability to reproduce the results of the FM depends on two thresholds and on the temperature at which the analyses are performed. The higher the threshold for the reaction rates analysis, the lower is the size of the RM and the higher the average error. The higher the threshold for the sensitivity analysis, the higher is the number of rate-limiting reactions and the better are the predictions of the RM in the negative temperature coefficient region. The best number of rate-limiting reactions was found equal to 500 for the two Curran's mechanisms. An RM generated at a high temperature has a smaller size and is more efficient in the high-temperature range than an RM generated at low temperature. However, it is unable to predict autoignition at low temperature.

Conversely, an RM generated at a low temperature has a larger size but is efficient at low and high temperature, provided the level of reduction is not too high. It is to be noted that the RMs are able to reproduce not only autoignition delay times but also species concentration profiles versus temperature obtained in JSR and VPFR studies.

RMs can facilitate the analysis of reaction flow, reaction path, and sensitivity used to interpret experimental results. They are suitably sized tools for one-dimensional flame calculations and are a good starting point for further reduction and multidimensional simulations.

The RMs for *n*-heptane and isooctane are available at the URL http://www-cms.llnl.gov/combustion/combustion2.html.

NOMENCLATURE

Symbol	Name
A_i	Pre-exponential factor of reaction i
E	Average error on the ignition delay time
ε_r	Rate threshold
FM	Full mechanism
G_{fast}	Group of fast reactions
$G_{\text{r}-1}$	Group of rate-limiting reactions
k	Index assigned to a reaction i according to the magnitude of $\overline{S_{\text{OH},i}}$
k_{cut}	Cutting rank
N_{r}	Number of reactions in the full mechanism
$N_{\text{r}-1}$	Number of rate-limiting reactions
N_{s}	Number of species in the full mechanism
r_i	Net rate of reaction i
$\overline{r_i(t)}$	Normalized rate of reaction i at time t
RM	Reduced mechanism
$S_{j,i}$	First-order local sensitivity coefficient of species j to reaction i
$\overline{S_{j,i}}$	log-Normalized sensitivity coefficient of species j to reaction i
$\overline{S_{\text{OH},i}}$	log-Normalized sensitivity coefficient of OH radical to reaction i
$\overline{S_{\text{OH},k}}$	log-Normalized sensitivity coefficient of OH radical to the reaction in kth position in the rank of coefficients $\overline{S_{\text{OH},i}}$ in decreasing order
t^*	Time at which the analysis of sensitivity is performed
T_{ana}	Analysis temperature
t_{ign}	Total ignition time
$Z_j(t)$	Mass fraction of species j at time t

This work was conducted in part under the auspices of the U.S. Department of Energy by the University of California, Lawrence Livermore National Laboratory, under Contract No. W-7405-Eng-48.

The authors acknowledge the computational center IDRIS of CNRS and especially Isabelle Dupays for her help and support.

BIBLIOGRAPHY

1. Smith, G. P.; Golden, D. M.; Frenklach, M.; Moriarty, N. W.; Eiteneer, B.; Goldenberg, M.; Bowman, C. T.; Hanson, R. K.; Song, S.; Gardiner, W. C., Jr.; Lissianski, V. V.; Qin, Z. http://www.me.berkeley.edu/gri_mech/.
2. Wilk, R. D.; Green, R. M.; Pitz, W. J.; Westbrook, C. K.; Addagarla, S.; Millze, D. L.; Cernansky, N. P. SAE 1990, Paper 900028.
3. Ribaucour, M.; Minetti, R.; Sochet, L. R.; Curran, H. J.; Pitz, W. J.; Westbrook, C. K. Proc Combust Inst 2000, 28, 1671–1678.
4. Curran, H. J.; Gaffuri, P.; Pitz, W. J.; Westbrook, C. K. Combust Flame 1998, 114, 149–177.
5. Curran, H. J.; Gaffuri, P.; Pitz, W. J.; Westbrook, C. K. Combust. Flame 2002, 129, 253–280.
6. Seiser, R.; Pitsch, K.; Seshhadri, K.; Pitz, W. J.; Curran, H. J. Proc Combust Inst 2000, 28, 2029–2037.
7. Løwås, T.; Amnéus, P.; Mauss, F.; Mastorakos, E. Proc Combust Inst 2002, 29, 1387–1393.
8. Tomlin, A. S.; Turanyi, T.; Pilling, M. J. In Low-Temperature Combustion and Autoignition, Comprehensive Chemical Kinetics; Compton, R. G.; Hancock, G. (Eds.); Elsevier: Amsterdam, 1997; Vol. 35, Ch. 4, pp. 293–437.
9. Griffiths, J. F. Prog Energy Combust Sci 1995, 21, 25–107.
10. Revel, J.; Boettner, J. C.; Cathonnet, M.; Bachman, J. S. J Chim Phys 1994, 91, 365–382.
11. Soyhan, H. S.; Mauss, F. Combust Sci Technol 2002, 174, 73–91.
12. Wang, H.; Frenklach, M. Combust Flame 1991, 87, 365–370.
13. Turányi, T. J Math Chem 1990, 5, 204–248.
14. Turányi, T. Reliability Eng Syst Saf 1997, 57, 41–48.
15. Vajda, S.; Valko, P.; Turányi, T. Int J Chem Kinet 1985, 17, 55–81.
16. Lu, T.; Law, C. K. Proc Combust Inst 2005, 30, 1333–1341.
17. Zheng, X. L.; Lu, T.; Law, C. K.; Westbrook, C. K.; Curran, H. J. Proc Combust Inst 2005, 30, 1101–1109.
18. Lu, T.; Law, C. K. Combust Flame 2006, 144, 24–36.
19. Pepiot, P.; Pittsh, H. In 4th Joint Meeting of the U.S. Sections of the Combustion Institute, Drexel University, March 21–23, 2005.
20. Bhattacharjee, B.; Schwer, D. A.; Barton, P. I.; Green, W. H. Combust Flame 2003, 135, 191–208.
21. Oluwole, O. O.; Bhattacharjee, B.; Tolsma, J. E.; Barton, P. I.; Green, W. H. Combust Flame 2006, 146, 348–365.

22. Tomlin, A. S.; Pilling, M. J.; Turányi, T.; Merkin, J. H.; Brindley, J. Combust Flame 1992, 91, 107–130.
23. Wang, W.; Rogg, B. In Lecture Notes in Physics; Springer-Verlag: Berlin, 1993; Vol. M15.
24. Lam, S. H.; Goussis, D. A. Proc Combust Inst 1988, 22, 931–941.
25. Tomlin, A. S.; Pilling, M. J.; Merkin, J. H.; Brindley, J.; Burgess, N.; Gough, A. Ind Eng Chem Res 1995, 34, 3749–3760.
26. Løwås, T.; Nisson, D.; Mauss, F. Proc Combust Inst 2000, 28, 1809–1815.
27. Turányi, T. Comput Chem 1994, 18, 45–54.
28. Mass, U.; Pope, S. B. Combust Flame 1992, 88, 239–264.
29. Conley, J. P.; Kazakov, A.; Dryer, F. L. In 3rd Joint Meeting of the U.S. Sections of the Combustion Institute, Book of Abstracts, PL06, Chicago, IL, March 2003.
30. Zhao, Z.; Conley, J. P.; Kazakov, A.; Frederick, L. D. SAE 2003, Paper 2003-01-3265.
31. Lutz, A. E.; Kee, R. J.; Miller, J. A. Sandia Report SAND87-8248, 1988.
32. Kee, R. J.; Rupley, F. M.; Miller, J. A. Sandia Report SAND89-8009B, 1991.
33. Nowak, U.; Warnatz, J. Prog Astronaut Aeronaut 1987, 113, 87–103.
34. Ray, W. J. Biochemistry 1983, 22, 4625–4637.
35. Minetti, R.; Ribaucour, M.; Carlier, M.; Fittschen, C.; Sochet, L. R. Combust Flame 1994, 96, 201–211.
36. Callahan, C. V.; Held, T. J.; Dryer, F. L.; Minetti, R.; Ribaucour, M.; Sochet, L. R.; Faravelli, T.; Gaffuri, P.; Ranzi, E. Proc Combust Inst 1996, 26,739–746.
37. Griffiths, J. F.; Halford-Maw, P. A.; Rose, D. J. Combust Flame 1993, 95, 291–306.
38. Minetti, R.; Carlier, M.; Ribaucour, M.; Therssen, E.; Sochet, L. R. Combust Flame 1995, 102, 298–309.
39. Dagaut, P.; Reuillon, M.; Cathonnet, M. Combust Sci Technol 1994, 95, 233–260.
40. Dagaut, P.; Reuillon, M.; Cathonnet, M. Combust Flame 1995, 101, 132–140.
41. Vermeer, D. J.; Meyer, J. W.; Oppenheim, A. K. Combust Flame 1972, 18, 327–336.
42. Coats, C. M.; Williams, A. Proc Combust Inst 1978, 17, 611–621.
43. Ciezki, H. K.; Adomeit, G. Combust Flame 1993, 93, 421–433.
44. Kee, R. J.; Rupley, F. M.; Miller, J. A.; Coltrin, M. E.; Grcar, J. F.; Meeks, E.; Moffat, H. K.; Lutz, A. E.; Dixon-Lewis, G.; Smooke, M. D.; Warnatz, J.; Evans, G. H.; Larson, R. S.; Mitchell, R. E.; Petzold, L. R.; Reynolds, W. C.; Caracotsios, M.; Stewart, W. E.; Glarborg, P.; Wang, C.; Adigun, O.; Houf, W. G.; Chou, C. P.; Miller, S. F. CHEMKIN Collection, Release 3.7, Reaction Design, Inc., San Diego, CA, 2002.
45. Fieweger, K.; Blumenthal, R.; Adomeit, G. Combust Flame 1997, 109, 599–619.